Characterization of a planar artificial magnetic metamaterial surface

D. R. Smith,* D. Schurig, and J. J. Mock
Department of Electrical and Computer Engineering, Duke University, Box 90291, Durham, North Carolina 27708, USA
(Received 22 December 2005; published 8 September 2006)

We explore the electromagnetic characterization of a planar artificial magnetic metamaterial. Because the composite structure is two- rather than three-dimensional, it does not form a medium with assignable bulk properties, such as the electric permittivity and magnetic permeability. However, we find that it is possible to characterize the expected bulk response of a structure composed of repeated layers of metamaterial planes, from a reflectance measurement of a single metamaterial surface made at an oblique angle. We present an analytical theory that relates the reflectance of a single plane to the expected bulk permeability and permeability of the composite, as well as supporting experiments and numerical simulations. Our results show that the recent use of reflectance measurements to characterize planar split ring resonator samples can reveal the presence of circulating currents in a sample—the precursor to artificial magnetism—but are insufficient to provide quantitative results unless the symmetry of the underlying metamaterial elements is carefully specified.

DOI: 10.1103/PhysRevE.74.036604 PACS number(s): 41.20.−q, 42.25.Bs, 78.20.−e

Artificially structured metamaterials have generated enormous interest for their ability to display electromagnetic responses unavailable in conventional materials [1]. Of particular interest has been the prospect of artificial magnetism, in which an array of patterned conducting elements can respond to an applied electromagnetic field with an effective permeability [2]. The patterned arrays in magnetic metamaterials are typically planar conducting split ring resonators (SRRs), in which circulating currents are induced in response to the incident time-varying magnetic field. SRRs are made resonant by the inclusion of a capacitive gap, enabling SRR structures to exhibit relatively large positive and negative values of effective permeability. Artificial magnetic metamaterials have enabled the development of negative index metamaterials, which require both the electric permittivity as well as the magnetic permeability to be less than zero [3–7].

Although the properties of SRRs have been well characterized at RF and microwave frequencies, several factors complicate the characterization of a metamaterial at higher frequencies. A major obstacle is the relative difficulty in obtaining phase information at frequencies above ~100 GHz. At low frequencies, vector network analyzers are widely available that provide accurate measurement of the phases and amplitudes of electromagnetic waves reflected from and transmitted through a finite thickness of metamaterial. From a measurement of these four quantities, the complex permittivity and permeability of a metamaterial can be determined [8,9]. In contrast, at higher frequencies the acquisition of phase information is less convenient. While techniques such as time-domain spectroscopy [10] or interferometry [11] can be applied to measure the transmitted or reflected phases, these techniques have not as yet been used to form a comprehensive characterization capability for metamaterials.

A second obstacle to the characterization of high-frequency metamaterials has been related to the geometry of samples that have typically been produced. To achieve the physical dimensions needed for structures designed to operate at wavelengths from submillimeter to the near infrared, advanced lithographic methods are required that often result in a single planar sample being available for proof-of-concept measurements [12–16]. A planar SRR sample for example, exhibits an anisotropic permeability in which the resonant component of the permeability tensor lies perpendicular to the plane. An electromagnetic wave directly incident on such a sample cannot sense the longitudinal magnetic response, unless there exists some magnetoelectric coupling to the transverse electric field. Such samples are properly described as *bianisotropic* and are inherently more electromagnetically complex than samples in which magnetoelectric coupling is absent.

In recent studies of high-frequency planar artificial magnetic structures, use has been made of magnetoelectric coupling to confirm the electromagnetic properties of the sample [15]. However, a quantitative measurement of the individual tensor components is not possible; rather, a normal incidence transmittance measurement (i.e., amplitude only) is performed and compared with the results of full-wave simulations to confirm the existence and location of the expected resonance. The character of the resonance—either electric or magnetic—is only known via the simulation results; direct incidence measurements on planar samples provide no specific value for the magnetic oscillator strength versus the electric oscillator strength. Nevertheless, these experiments have successfully demonstrated that high-frequency SRRs can support circulating currents, indicating the likelihood that these materials also exhibit artificial magnetism [15,16].

By stacking multiple layers of a planar sample, it is possible to obtain a large enough structure to perform normal incidence measurements in the propagation direction parallel to the plane. This technique has been used very recently in the characterization of an artificial magnetic structure at terahertz frequencies [17]. Since the wave in this configuration directly senses the magnetic response of the SRRs, the structure can be designed without magnetoelectric coupling and the complexity of the measurement is significantly reduced. However, the assembly of multilayer structures is not always convenient for the high frequency SRR layers.

Additional information regarding the magnetic response

*Email address: drsmith@ee.duke.edu

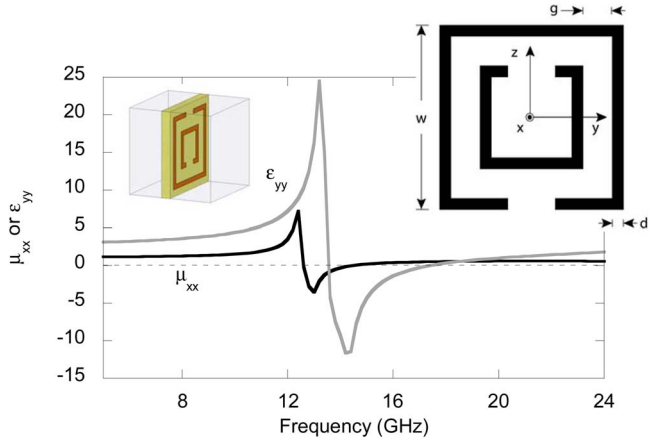

FIG. 1. (Color online) The real part of μ_{xx} (black curve) and ε_{yy} (gray curve) for the symmetric SRR medium. (Inset, left) The unit cell of the SRR medium used in the simulations and measurements. (Inset, right) The SRR dimensions are $w=2.0$ mm, $d=0.13$ mm, $g=0.35$ mm. The gaps in the rings are 0.47 mm. The substrate is FR-4 circuit board material, 0.25 mm thick with dielectric constant of 3.75. The unit cell is cubic, with length 2.4 mm.

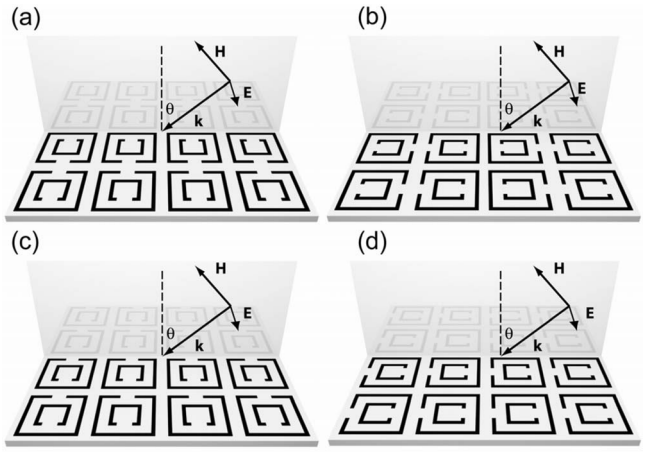

FIG. 2. An oblique *S*-polarized wave incident on different planar SRR media. (a) The wave is oriented relative to a symmetric SRR medium so that the magnetic response is maximized (magnetic configuration); (b) the wave is oriented relative to a symmetric SRR medium so as to excite the resonant electric response in addition to the magnetic response (electric configuration); (c) the magnetic configuration for an asymmetric SRR medium; and (d) the electric configuration for an asymmetric SRR medium.

of planar SRR samples can be obtained by a series of reflectance measurements with waves incidents at a series of oblique angles relative to the surface normal of the SRR plane. Such an *ellipsometric* approach was proposed as a means of characterizing the artificial magnetism of planar SRRs at terahertz frequencies [12]. However, the complicated electromagnetic nature of the anisotropic planar SRR sample makes ellipsometry difficult to pursue in general. Our goal here is to show that by increasing the symmetry of the fabricated SRR structure, direct signatures of the artificial magnetic oscillator response can be obtained without the full complexity that ellipsometry entails.

The SRR is inherently bianisotropic, exhibiting both electric and magnetic coupling as well as magnetoelectric coupling to the incident field. When assembled into a medium, the composite can be described by the constitutive relations

$$\mathbf{D} = \varepsilon_0 \boldsymbol{\varepsilon} \mathbf{E} + i\sqrt{\varepsilon_0 \mu_0}\boldsymbol{\kappa}\mathbf{H},$$

$$\mathbf{B} = -i\sqrt{\varepsilon_0 \mu_0}\boldsymbol{\kappa}^T\mathbf{E} + \mu_0 \boldsymbol{\mu}\mathbf{H}. \tag{1}$$

Assuming axes fixed to the SRR as shown in the inset to Fig. 1, a general analysis reveals that the SRR medium can be approximately described by the following generic material parameters [18,19]

$$\varepsilon_{zz} = a, \quad \varepsilon_{yy} = a + \frac{b\omega^2}{(\omega_0^2 - \omega^2)},$$

$$\mu_{xx} = 1 + \frac{c\omega^2}{(\omega_0^2 - \omega^2)}, \quad \kappa_{xy} = \frac{d\omega\omega_0}{(\omega_0^2 - \omega^2)}. \tag{2}$$

Padilla has recently presented an analysis based on group theory in which the symmetry of the SRR medium is related to the available electromagnetic modes and their corresponding field and current distributions [20]. In this analysis, symmetry is used to determine which of the electromagnetic material parameters will be nonzero for a particular lattice configuration. Based on these symmetry arguments it can be understood that the magnetoelectric coupling term, κ_{xy}, can be made negligible by orienting neighboring SRRs such that a mirror symmetry exists about the principal axes in the plane, as pointed out earlier by Marqués *et al.* [18]; however, a coexistent resonant electric response is unavoidable so long as the SRR itself breaks symmetry. This is illustrated by the retrieved material parameters obtained from an *S*-parameters simulation on the specific SRR structure shown in the inset to Fig. 1 [8]. A combination of electric and magnetic boundary conditions on the unit cell has been employed so that the composite structure modeled has reflection symmetry in the SRR plane [see Fig. 2(a)]. The *S*-parameters retrieval yields the expected resonant forms for μ_{xx} and ε_{yy} as shown. What is notable is that, for this structure, the strength of the resonance of ε_{yy} is much larger than that of μ_{xx}, a characteristic that is even more pronounced in higher frequency SRR samples [12–17].

To gain some insight into the scattering properties of oblique reflectance from a planar sample, we first consider a simple analytical model. The reflection coefficient for an *S*-polarized (or TE) wave incident obliquely on the planar SRR sample as in Fig. 2(a) has the form

$$r_S = \frac{-\frac{1}{2}i\left(\frac{k\mu_y}{q} - \frac{q}{k\mu_y}\right)\sin(qd)}{\cos(qd) - \frac{i}{2}\left(\frac{k\mu_y}{q} + \frac{q}{k\mu_y}\right)\sin(qd)}, \tag{3}$$

where $k_0 = \omega/c$, $k = \sqrt{k_0^2 - k_y^2}$, $q = \sqrt{\mu_y \varepsilon_z k_0^2 - \frac{\mu_y}{\mu_x}k_y^2}$, and d is the thickness of the plane. r_s relates the reflected electric field amplitude $\mathbf{E}_r$ to the incident electric field amplitude $\mathbf{E}_i$, according to $\mathbf{E}_r = r_s \mathbf{E}_i$. We choose to examine the obliquely

incident *S*-polarized waves because the magnetic field for these waves possesses a component that can excite the SRRs. We can safely assume that there is no magnetic polarizability in the (yz) SRR plane since no solenoidal currents can be generated that would flow out of the SRR plane; thus, $\mu_y = 1$. For the symmetric SRR structure, only the normal component of μ (μ_x) and one of the transverse components of ε (ε_y) will be non-negligible near resonance.

For a single planar layer of SRRs, the physical thickness of the layer is extremely small, usually many times smaller than the wavelength. We thus take the limit $qd \ll 1$ in Eq. (3) in such a way that as $k_0 d \to 0$, $\varepsilon_y' = \varepsilon_y k_0 d$, and $\mu_x' = \mu_x / k_0 d$ remain finite. These limits can be understood as resulting from the requirement that the depolarizing charges induced on the (infinitesimally thin) slab remain finite. Applying the $d \to 0$ limit, we find for the configuration shown in Fig. 2(a)

$$r_S = \frac{-i \sin^2 \theta}{2\mu_x' \cos \theta - i \sin^2 \theta}, \tag{4}$$

where θ is the angle of incidence. For the configuration shown in Fig. 2(b), the incident wave presumably induces both a magnetic as well as an electric dipole response; however, given the relative oscillator strengths as shown in Fig. 1, we expect the electric response to dominate, in which case Eq. (3) reduces to

$$r_S = \frac{-i\varepsilon_y'}{2 \cos \theta - i\varepsilon_y'}. \tag{5}$$

Note that the approximation that leads to Eqs. (4) and (5) is at odds with the usual metamaterials picture in which the *effective* thickness d of the layer is much larger, usually on the order of the unit cell size rather than the infinitesimal limit we have used here. Both approaches should be valid depending on the context. Because a single layer of SRRs does not necessarily constitute an effective medium normal to the plane, a description in terms of the induced electric and magnetic polarizations is actually more appropriate than one of permittivity and permeability. Such a description for metamaterial interfaces has been developed by Kuester *et al.* [21]; we expect the two descriptions to be equivalent.

For a resonant longitudinal permeability, Eq. (4) shows that the reflection coefficient will exhibit a minimum *at the peak of the resonance*, while for a resonant planar permittivity, Eq. (5) shows that the reflection coefficient is a minimum *where the permittivity passes through zero*. In what follows, we will refer to the SRR structure and orientation of the incident wave shown in Figs 2(a) and 2(b) as symmetric/magnetic and symmetric/electric. In both configurations the incident wave excites the magnetic dipole, but it only excites the electric dipole in the symmetric/electric configuration.

To verify the predictions of our approximate model, we first perform a numerical simulation of the specular scattering of an obliquely incident wave on the planar structure shown in Fig. 2, using a finite-difference time-domain (FDTD) numerical procedure described elsewhere [22]. We plot in Fig. 3 the reflectance of a wave incident on the symmetric SRR configuration at 60° to the surface normal for both the symmetric/magnetic and symmetric/electric configurations of Figs. 2(a) and 2(b). A comparison between Figs. 1 and 3 shows that the simulated reflectance confirms the qualitative predictions of our simple analytical model. For the SRRs in the magnetic configuration, a minimum in the reflectance occurs near 14 GHz, while for the SRRs in the electric configuration a dip occurs near 20 GHz. Note the presence of a small dip near 14 GHz in the electric SRR configuration; this dip results from the magnetic response of the SRR, neglected in Eq. (5). The magnetic response can be seen to be a relatively minor perturbation relative to the dominant electric response, justifying our approximations above. Note that there is a considerable offset in the apparent positions of the magnetic and electric resonances in Fig. 3 versus those found by the retrieval in Fig. 1. This difference is presumably due to the interaction between planes of SRRs in the latter case, which causes a frequency shift in the effective medium parameters.

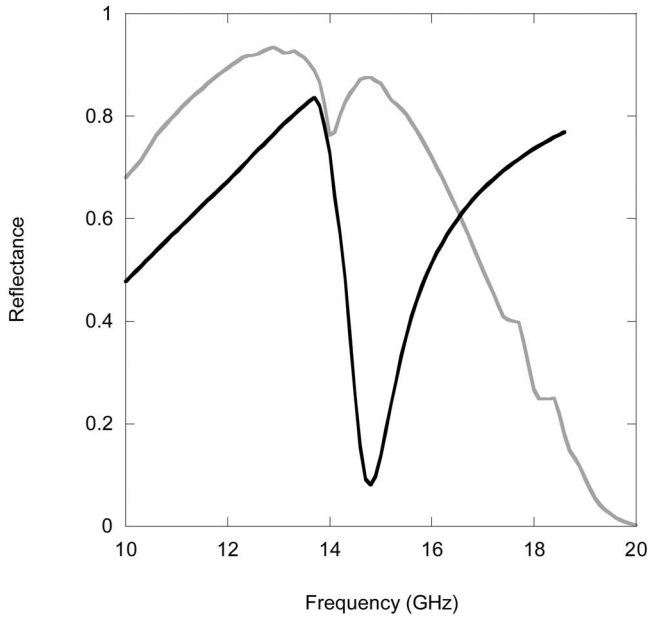

FIG. 3. Numerically computed reflectance for a wave incident on the planar symmetric SRR medium, 60° to the surface normal. Both the magnetic (black curve) and electric (gray curve) configurations are shown.

The analytic results above, confirmed by the curves obtained in Fig. 3, illustrate that the presence of what appears to be a resonance (or dip) in the reflectance is an unreliable predictor of the resonant frequency of the planar structure and whether the underlying response is electric or magnetic. Additional information as to the orientation *and symmetry* of the sample plane must be supplied to make a single reflectance measurement meaningful. For cases where the sample plane symmetry is known in advance, Fig. 3 indicates that reflectance measurements can be useful to confirm global features of the planar SRR sample properties.

While the primary interest in oblique reflectance measurements is the characterization of samples designed to operate at higher (>100 GHz) frequencies, we find it convenient here to confirm the nature of these reflectance simulations in analog experiments performed at microwave frequencies. The constituent materials used to form the samples (e.g.,

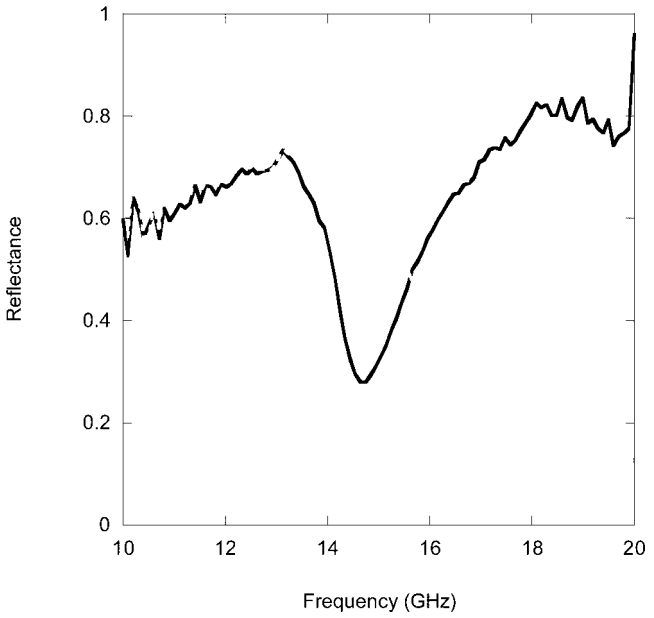

FIG. 4. Measured reflectance for a wave incident on the planar SRR medium, 60° to the surface normal. Both the magnetic (solid black curve) and electric (solid gray curve) configurations are shown for the symmetric sample, as well as the electric configuration for the asymmetric sample (dashed gray curve).

circuit board, copper) are all well characterized at microwave frequencies, eliminating possible ambiguities that may arise from dispersive substrate materials and so forth that occur at terahertz and higher frequencies [12].

Using an optical lithography procedure previously described [23], we fabricated planar SRR samples of the design shown in Fig. 1. Three planar samples were produced: symmetrized SRRs, as in Figs. 2(a) and 2(b); asymmetric SRRs (gaps all oriented in the same manner), as in Figs. 2(c) and 2(d); and SRRs with the gaps in the rings closed. The latter sample was used as a control to confirm the observed resonant response was correlated with the presence of the gaps in the rings.

A pair of polarized, focused horn/lens assemblies (Rozendal Associates, El Cajon, California) was used to excite and detect microwave radiation. The focal length of each horn is 30 cm, with a focal spot size of roughly 4 cm. The frequency range of the horns is 12–20 GHz, although we find that useful data can be obtained down to a frequency of 10 GHz. The horns were positioned 30 cm away from the sample plane, at an angle of 60° on either side of the surface normal. Data was taken with the horns oriented for *S* polarization, and for the two relevant rotations of the samples. In the case of the symmetrized SRRs, two orientations of the SRR structure were measured, corresponding to those illustrated in Figs. 2(a) and 2(b). In the case of the asymmetric SRR samples, cross polarization was also measured.

The results of the measurements on the symmetric samples are shown in Fig. 4. Very good agreement is seen between the measured data and the simulated structure (Fig. 3), both of which are consistent with the simple model of Eqs. (4) and (5). The agreement between simulation and measurement in particular suggests the possibility of formulating a more rigorous characterization of high frequency metamaterial samples by reflectance measurements, so long as the sample is symmetrized as in Figs. 2(a) and 2(b). Because of the underlying symmetry of the symmetric/magnetic structure, for example, we can state unambiguously that the observed dip occurs at the resonance frequency of the SRR material and that the depth of the dip provides information on the magnetic oscillator strength.

When the SRR sample is asymmetric, magnetoelectric coupling cannot be neglected and the form for the reflectance becomes significantly more complicated, potentially coupling both *S* and *P* polarizations. Given that the reflectance is generally a function of both resonant components and the cross coupling term $\boldsymbol{\kappa}_{xy}$ for an asymmetric SRR sample, the only information that can be obtained from a single oblique reflectance measurement is the existence of a material resonance. Even were it possible to obtain complex transmission and reflection coefficients, the resulting four quantities would be insufficient to characterize a sample having six unknown quantities (i.e., ε, μ, and κ).

For the purposes of illustration, we can consider the electric coupling case of Fig. 1(d). If we solve for the *x* component of the wave vector for an *S*-polarized wave within the material, we find (ignoring all nonresonant terms)

$$q_x^2 = \left(\varepsilon_y - \frac{\kappa_{yx}^2}{\mu_x}\right)k_0^2 - \frac{k_y^2}{\mu_x}. \tag{6}$$

The corresponding field solutions maintain orthogonality between *S* and *P* polarization so that no polarization conversion occurs. We can write the reflection coefficient in the $k_0 d \rightarrow 0$ limit as

$$r_S = \frac{-i\left(\varepsilon_y' - \frac{\kappa_{yx}^2}{\mu_x'} - \frac{\sin^2\theta}{\mu_x'}\right)}{2\cos\theta - i\left(\varepsilon_y' - \frac{\kappa_{yx}^2}{\mu_x'} - \frac{\sin^2\theta}{\mu_x'}\right)}. \tag{7}$$

Equation (6) predicts maximum reflectance at resonance, with no particular dips (due to a zero in the numerator or pole in the denominator) as in the symmetric SRR cases. The analogous reflectance measurement on the fabricated asymmetric SRR sample shows this expected behavior (Fig. 4, dashed gray line).

The second asymmetric orientation, the magnetic asymmetric case shown in Fig. 2(c), proves to be the most difficult to analyze, and we only make some general observations here. The derived expression for q_z within the material is much more complicated than the previous expressions; an analysis of the corresponding reflected field solutions reveals them to be elliptically polarized. Thus, we expect the reflectance spectrum corresponding to the magnetic asymmetric configuration to exhibit polarization conversion. Cross-polarization was measured for all of the SRR samples; only the magnetic asymmetric configuration displayed significant cross-polarization, 20–30 dB above the noise floor of our network analyzer.

We have presented an analysis of the oblique reflectance properties of planar SRR samples with varying symmetry.

We find that the bianisotropy inherent to the asymmetric SRR design leads to considerable complication in the interpretation of reflectance data. This complication is not in principle insurmountable; recently, Grzegorczyk *et al.* [24] have presented a complete retrieval algorithm, applicable to an arbitrary bianisotropic material, based on a combination of reflectance and transmittance measurements at many angles of incidence. While this approach is in principle complete, it necessitates the collection of numerous data sets and requires extensive analysis that may be subject to numerical instability in practical applications.

When the SRR sample can be fabricated so as to eliminate on average mirror asymmetry in the plane, the reflectance properties are more easily related to the nonvanishing material parameters. We find that characteristic forms for the reflectance are obtained, which can be used to make definitive statements regarding the magnetic or electric properties of the sample. We will pursue the quantitative retrieval of the effective medium parameters from a reduced set of reflectance measurements on a symmetrized SRR sample in a future publication.

ACKNOWLEDGMENTS

This work was supported by DARPA (Contract No. HR0011–05–3–0002). D. Schurig also acknowledges support from the IC Postdoctoral Fellowship Program.

[1] J. B. Pendry and D. R. Smith, Phys. Today **57**, 37 (2004).
[2] J. B. Pendry, A. J. Holden, D. J. Robbins, and W. J. Stewart, IEEE Trans. Microwave Theory Tech. **47**, 2075 (1999).
[3] D. R. Smith, W. J. Padilla, D. C. Vier, S. C. Nemat-Nasser, and S. Schultz, Phys. Rev. Lett. **84**, 4184 (2000).
[4] A. A. Houck, J. B. Brock, and I. L. Chuang, Phys. Rev. Lett. **90**, 137401 (2003).
[5] C. G. Parazzoli, R. B. Greegor, K. Li, B. E. C. Koltenbah, and M. Tanielian, Phys. Rev. Lett. **90**, 107401 (2003).
[6] C. G. Parazzoli, R. B. Greegor, J. A. Nielsen, M. A. Thompson, K. Li, A. M. Vetter, M. H. Tanielian, and D. C. Vier, Appl. Phys. Lett. **84**, 3232 (2004).
[7] R. W. Ziolkowski, IEEE Trans. Antennas Propag. **51**, 1516 (2003).
[8] D. R. Smith, S. Schultz, P. Markos, and C. M. Soukoulis, Phys. Rev. B **65**, 195104 (2002).
[9] S. He, Z. Ruan, L. Chen, and J. Shen, Phys. Rev. B **70**, 115113 (2004).
[10] D. Grischkowsky, S. Keiding, M. Van Exter, and Ch. Fattinger, J. Opt. Soc. Am. B **7**, 2006 (1990).
[11] V. M. Shalaev, W. Cai, U. Chettiar, H.-K. Yuan, A. K. Sarychev, V. P. Drachev, and A. V. Kildishev, *Negative Index of Refraction in Optical Metamaterials*, LANL Server physics/0504091.
[12] T. J. Yen, W. J. Padilla, N. Fang, D. C. Vier, D. R. Smith, J. B. Pendry, D. N. Basov, and X. Zhang, Science **303**, 1494 (2004).
[13] H. O. Moser, B. D. F. Casse, O. Wilhelmi, and B. T. Saw, Phys. Rev. Lett. **94**, 063901 (2005).
[14] S. Zhang, W. Fan, B. K. Minhas, A. Frauenglass, K. J. Malloy, and S. R. J. Brueck, Phys. Rev. Lett. **94**, 037402 (2005).
[15] K. Aydin, K. Guven, M. Kafesaki, L. Zhang, C. M. Soukoulis, and E. Ozbay, Opt. Lett. **29**, 2623 (2004).
[16] S. Linden, C. Enkrich, M. Wegener, J. F. Zhou, T. Koschny, and C. M. Soukoulis, Science **306**, 1351 (2004).
[17] N. Katsarakis, G. Konstantinidis, A. Kostopoulos, R. S. Penciu, T. F. Gundogdu, M. Kafesaki, E. N. Economou, Th. Koschny, and C. M. Soukoulis, Opt. Lett. **30**, 1348 (2005).
[18] R. Marqués, F. Medina, and R. Rafii-El-Idrissi, Phys. Rev. B **65**, 144440 (2002).
[19] R. Marqués, F. Mesa, J. Martel, and F. Medina, IEEE Trans. Antennas Propag. **51**, 2572 (2003).
[20] W. Padilla, "Group theoretical description of artificial magnetic metamaterials utilized for negative index of refraction," http://xxx.lanl.gov/abs/physics/0508307.
[21] E. F. Kuester, M. A. Mohamed, M. Piket-May, and C. L. Holloway, IEEE Trans. Antennas Propag. **51**, 2641 (2003).
[22] D. Schurig, Int. J. Numer. Model. **19**, 215 (2006).
[23] J. N. Gollub, D. R. Smith, D. C. Vier, T. Perram, and J. J. Mock, Phys. Rev. B **71**, 195402 (2005).
[24] T. Grzegorczyk *et al.* (private communication).